Published in final edited form as:
J Immunol. 2008 January 1; 180(1): 590–600.

Integrin $\alpha_D\beta_2$ Is Dynamically Expressed by Inflamed Macrophages and Alters the Natural History of Lethal Systemic Infections[1]

Yasunari Miyazaki[*,2,3], **Michaeline Bunting**[*,2,4], **Diana M. Stafforini**[†,‡], **Estelle S. Harris**[*,‡], **Thomas M. McIntyre**[‡,§,5], **Stephen M. Prescott**[†,‡,6], **Valber S. Frutuoso**[¶], **Fabio C. Amendoeira**[¶], **Danielle de Oliveira Nascimento**[¶], **Adriana Vieira-de-Abreu**[¶], **Andrew S. Weyrich**[*,‡], **Hugo C. Castro-Faria-Neto**[¶], and **Guy A. Zimmerman**[*,‡,7]

* *Program in Human Molecular Biology and Genetics, University of Utah, Salt Lake City, UT 84112*

† *Huntsman Cancer Institute, University of Utah, Salt Lake City, UT 84112*

‡ *Department of Internal Medicine, University of Utah, Salt Lake City, UT 84112*

§ *Department of Pathology, University of Utah, Salt Lake City, UT 84112*

¶ *Laboratório de Immunofarmacologia, Departmento de Fisiologia e Farmacodinamica, Instituto Oswaldo Cruz, Fundacão Oswaldo Cruz, Rio de Janeiro, Brazil*

Abstract

The leukocyte integrins have critical roles in host defense and inflammatory tissue injury. We found that integrin $\alpha_D\beta_2$, a novel but largely uncharacterized member of this family, is restricted to subsets of macrophages and a small population of circulating leukocytes in wild-type mice in the absence of inflammatory challenge and is expressed in regulated fashion during cytokine-induced macrophage differentiation in vitro. $\alpha_D\beta_2$ is highly displayed on splenic red pulp macrophages and mediates their adhesion to local targets, identifying key functional activity. In response to challenge with *Plasmodium berghei*, a malarial pathogen that models systemic infection and inflammatory injury, new populations of $\alpha_D{}^+$ macrophages evolved in the spleen and liver. Unexpectedly, targeted deletion of α_D conferred a survival advantage in *P. berghei* infection over a 30-day observation period. Mechanistic studies demonstrated that the increased survival of $\alpha_D{}^{-/-}$ animals at these time points is not attributed to differences in magnitude of anemia or parasitemia or to alterations in splenic microanatomy, each of which is a key variable in the natural history of *P. berghei* infection, and indicated that an altered pattern of inflammatory cytokines may contribute to the difference in mortality. In contrast to the outcome in malarial challenge, death of $\alpha_D{}^{-/-}$ animals was accelerated in a model of *Salmonella* sepsis, demonstrating differential rather than stereotyped roles for $\alpha_D\beta_2$ in

[1]This work was supported by National Institutes of Health Grant HL44525 (to G.A.Z.), a National Institutes of Health Special Center of Research in Acute Respiratory Distress Syndrome (P50 H150153), an Asthma Research Center Award funded by the American Lung Association, the Margolis Foundation, and an Established Investigator Award from the American Heart Association (to A.S.W.).

[7] Address correspondence and reprint requests to Dr. Guy A. Zimmerman, Program in Human Molecular Biology and Genetics, University of Utah, 15 North 2030 East, Building 533, Room 4220, Salt Lake City, UT 84112. E-mail address: guy.zimmerman@hmbg.utah.edu.

[2]Y.M. and M.B. contributed equally to this work. M.B. accomplished cloning of the mouse α_D gene, generation of α_D-deficient animals, initial genotype-phenotype correlation, and development of in vitro models of α_D expression. Y.M. performed extensive characterization of $\alpha_D\beta_2$ in murine tissues and additional genotype-phenotype correlation, developed in vitro models of cellular adhesion, characterized α_D expression in in vivo disease models, and compiled major portions of the manuscript text.

[3]Current address: Department of Integrated Pulmonology Medicine, Tokyo Medical and Dental University, 1-5-45 Yushima Bunkyo-Ku, Tokyo, Japan, 233-0015.
[4]Current address: Invitrogen Corporation, 1610 Faraday Avenue, Carlsbad, CA 92008.
[5]Current address: Department of Cell Biology, NN1-28, Lerner Research Institute, Cleveland, OH 44195.
[6]Current address: Oklahoma Medical Research Foundation, 825 Northeast 13th Street, Oklahoma City, OK 73104.

Disclosures
The authors have no financial conflict of interest.

systemic infection. These studies identify previously unrecognized and unique activities of $\alpha_D\beta_2$, and macrophages that express it, in host defense and injury.

Integrins are plasma membrane heterodimers that are broadly distributed on metazoan cells and mediate critical functions, including adhesion, homing, signaling, and gene expression. The leukocyte integrin subfamily (also called β_2 or CD11/CD18 integrins) is expressed on myeloid and lymphoid leukocytes and their precursors and consists of four members (1): $\alpha_L\beta_2$ (CD11aCD18; LFA-1), $\alpha_M\beta_2$ (CD11b/CD18; MAC-1; CR3), $\alpha_x\beta_2$ (CD11c/CD18), and $\alpha_D\beta_2$ (CD11d/CD18). Leukocyte integrins are required for host defense against invasion by many pathogens and for wound surveillance and repair, demonstrated by heritable deficiency syndromes that cause recurrent and often life-threatening infections in humans and domesticated animals (2). Experimental models in which leukocyte integrins are genetically deleted or are blocked demonstrate critical and complex activities relevant to this function (1,3–6). In contrast, unregulated accumulation and signaling of leukocytes mediated by β_2 integrins also contribute to inflammatory tissue injury (1,2,6,7).

Integrin $\alpha_D\beta_2$ is the most recently discovered β_2 integrin (1,8). Molecular characterization of the α_D subunit suggested that $\alpha_D\beta_2$ has novel activation pathways and modes of regulation (8). $\alpha_D\beta_2$ recognizes ICAM-3, VCAM-1, and several other ligands in assays with primary and surrogate cells (8–11), although adhesive interactions in vivo have not been identified. Sequence similarity of the I domains of α_D and α_M (8) predicted this diversity in ligand recognition: the I domain is critical in binding interactions of integrins, and $\alpha_M\beta_2$ also has multiple ligand partners in experiments using transfected cell lines (1,10,11). Limited observations suggest that $\alpha_D\beta_2$ is preferentially expressed by macrophages in normal human tissues and in clinical syndromes of dysregulated inflammation, including atherosclerosis, rheumatoid arthritis, and acute lung inflammation (Refs. 8,12, and 13 and our unpublished data), and that it is involved in immune regulation and inflammatory tissue injury in rodent models (14–16). Nevertheless, the distribution, regulation, and activities of $\alpha_D\beta_2$ in physiologic and pathologic inflammation are largely undefined, and phenotypes in mice made genetically deficient in α_D have not been reported (1,3,16). In this study, we examined the expression and functions of $\alpha_D\beta_2$ in naive conditions and in response to inflammatory stimulation in models of pathologic infectious syndromes. We found that it is selectively expressed by subsets of splenic red pulp, thymic, and marrow macrophages in wild-type (WT)[8] animals in the basal state. This pattern of expression suggested roles in systemic infectious challenge. We found that new populations of α_D^+ macrophages emerge in response to infection with *Plasmodium berghei*, a blood-borne malarial protozoan recognized by splenic red pulp macrophages, demonstrating that $\alpha_D\beta_2$ is dynamically modulated in systemic inflammation. Targeted deletion of α_D did not cause a spontaneous phenotype but, unexpectedly, conferred a survival advantage in lethal *P. berghei* infection. In contrast, deletion of $\alpha_D\beta_2$ reduced survival in animals infected with *Salmonella typhimurium*, an intracellular bacterial pathogen that also causes a lethal systemic infection in mice and is recognized by splenic marginal zone macrophages and other macrophage subsets. Our findings demonstrate unique functional roles for $\alpha_D\beta_2$ and the macrophage populations that express it in innate responses to microbial invasion and systemic infectious syndromes.

[8]Abbreviations used in this paper: WT, wild type; PRBC, parasitized RBC; iNOS, inducible NO synthase.

Materials and Methods

Targeting vector construction, functional disruption of α_D by homologous recombination, and generation of $\alpha_D^{-/-}$ mice

Genomic clones were isolated from a murine 129Sv genomic library using probes specific for the α_D I domain, which is critical for ligand recognition (1,10,11), and targeted deletion of α_D was accomplished using previously described strategies (17–19) (Fig. 1).

Immunohistochemistry

The following were used as primary mAbs in immunocytochemical reactions: α_D, 205c, and 279F (hamster IgG; ICOS) (14); F4/80, A3-1 (rat IgG2; Serotec); MARCO, ED31 (rat IgG1; Serotec); and MOMA-1 (rat IgG2; Serotec) (20). Tissues from various organs, usually from 8- to 12-wk-old animals in studies of distribution of $\alpha_D\beta_2$ in WT mice, were frozen in Tissue-Tek (Sakura Finetek) and 8-μm cryostat sections were deposited on Superfrost Plus slides (Fisher Scientific). The sections were then fixed in cold acetone for 10 min. Immunoperoxidase staining was based on a previously described method (21) (Fig. 2). For immunofluorescent staining, sections were blocked with 5% normal goat serum, 1% BSA, and avidin solution (Vector Laboratories) for 30 min and subsequently incubated with primary Abs overnight at 4°C. Biotin-conjugated goat anti-hamster Ab was applied at a 1/1000 dilution and incubated for 30 min followed by incubation with Alexa 488-conjugated streptavidin and Alexa 568-conjugated anti-rat IgG (Molecular Probes) for 45 min. The sections were then layered with anti-fade medium (Biomeda) and sealed with a coverslip. Fluorescent staining was analyzed using a FluoView 300 microscope (Olympus) in the University of Utah Health Science Center's Core Cell Imaging Facility.

Isolation of mouse splenocytes and F4/80-positive splenic macrophages

Single-cell suspensions from freshly isolated spleen were obtained as described previously (22), with minor modifications. F4/80-positive splenic macrophages were further isolated using an AutoMACS cell sorter and positive selection using PE-conjugated anti-F4/80 Ab (Serotec) and anti-PE magnetic beads according to the manufacturer's instructions (Miltenyi Biotec).

Flow cytometric analysis

Isolated F4/80-positive splenocytes or cultured M1 cells were incubated on ice for 30 min in the presence of Alexa 488-conjugated mAb 205c or a control Ab. Cells were washed with FACS medium (HBSS without Ca^{2+} and Mg^{2+}/0.1% NaN_3/0.5% human serum albumin) and fixed in 1% paraformaldehyde. They were then analyzed by flow cytometry as previously described (23), with minor modifications.

Culture of murine M1 cells

The murine M1 myeloid leukemic cell line was obtained from American Type Culture Collection. Macrophage differentiation was induced as described elsewhere (24). PCR assays for α_D mRNA were done essentially as described previously (17). The primers used (5′-CAATCCCTGCTACCATGCCAGA-3′ and 5′-CTCCTGTAGGGCAGTGGGTTC-3′) amplified a 490-bp product. Immunocytochemical analysis was accomplished as previously outlined (25).

Modified Stamper-Woodruff adhesion assay

An assay for in vitro binding of splenic macrophages to freshly isolated spleen sections was developed based on previously described methods (26,27). All steps were conducted in a cold room or on ice. Incubations were done using freshly cut, unfixed, 10-μm sections of WT or

α_D knockout spleen prepared using a cryostat (Leica CM 3050). F4/80-positive splenocytes were prepared and labeled with PE, suspended in RPMI 10 at a final concentration of 1×10^7 cells/ml, and layered over each section. The slides were immediately placed on a rotating platform at 60 rpm. After incubation for 30 min, the sections were washed by dipping the slides repeatedly in cold PBS and fixed for 10 min in 2% paraformaldehyde at 4°C. The sections were then washed again and mounted on glass slides with anti-fade medium. Images of the adherent PE-positive cells detected by fluorescent microscopy were captured and analyzed using a FluoView 300 microscope and the number of PE-positive cells bound to each section was counted using NIH ImageJ.

Characterization of $\alpha_D\beta_2$-deficient and WT mice in models of systemic infectious challenge

The experiments in these studies were approved by the Animal Welfare Committee of the Oswaldo Cruz Institute and by the University of Utah Animal Care and Use Committee. C57BL/6 WT and $\alpha_D^{-/-}$ mice from the Oswaldo Cruz Foundation breeding unit weighing 20–25g were used for most studies. A/J, SJL/J, and Swiss mice from B&K were also used in some experiments. The animals were kept at constant temperature (25°C) with free access to chow and water in a room with a 12-h light/dark cycle.

C57BL/6 mice were infected by an i.p. injection of 200 μl of PBS containing 10^5 RBC parasitized with the Pasteur strain of *P. berghei* ANKA (28). In parallel experiments, we established that this inoculum is lethal in a high percentage of animals after 20–30 days of infection, consistent with studies using other *P. berghei* strains (29). Samples of spleen and liver were obtained at different times postinfection of WT mice after sacrificing the animals in a CO_2 chamber. The tissue was frozen and later analyzed by immunohistochemistry. For survival studies, groups of 10 WT and 10 $\alpha_D^{-/-}$ mice were studied together. Surviving animals were sacrificed at 30 days postinfection. The numbers of parasitized RBC and the hematocrits were determined as previously described (28) in separate groups of animals.

For studies of *Salmonella* infection, *Salmonella enterica* serovar *typhimurium* ISC 5302/2004, a generous gift from the Department of Microbiology of the Instituto Oswaldo Cruz, was cultured in Luria-Bertani broth (Guria Broth Miller; Sigma-Aldrich) for 16–18 h at 37°C to obtain stationary growth phase cultures. The bacteria were then centrifuged (200 rpm) for 10 min at 4°C and the pellets were resuspended in PBS to an OD of 0.1 at 660 nm, corresponding to 10^8 CFU/ml. WT and $\alpha_D^{-/-}$ mice were infected by i.p. injection of 200 μl of bacterial suspension (10^5 CFU/mouse). Control WT mice were sham injected (saline alone) in parallel. Survival was monitored for 10 or 15 days, at which time animals remaining alive were sacrificed.

Log rank tests were used for comparison of Kaplan-Meier survival plots in studies of *P. berghei* and *Salmonella* infection. A $p \leq 0.05$ was considered statistically significant for differences in the mortality data.

Multiplex cytokine and IL-12 determinations

Initial screening analysis of multiple cytokines in the serum of three $\alpha_D^{-/-}$ and three WT mice was done using a Luminex system (Bio-Plex; Bio-Rad). Subsequent measurements of IL-12 (p40) levels in samples from larger groups of $\alpha_D^{-/-}$ and WT animals were done by commercial ELISA according to the manufacturer's instructions (R&D Systems). Differences in mean IL-12 levels were examined by one-way ANOVA.

Results

Generation and characterization of α_D knockout mice

α_D-deficient ($\alpha_D^{-/-}$) mice were generated by targeted deletion of the I domain and excision of the "floxed" selection cassette to avoid spurious in vivo consequences (Ref. 17 and Fig. 1). Progeny containing the α_D^{loxP} allele were backcrossed and maintained on the C57BL/6 background. Heterozygous and homozygous animals were born at expected Mendelian ratios and did not display gross physical abnormalities. Homozygous animals were fertile and did not have an increased incidence of spontaneous infection. Leukocyte counts and morphology were similar between WT and homozygous mutant animals. The mean weight of spleens from 10-to 11-wk-old $\alpha_D^{-/-}$ mice was greater than that of WT animals (105 vs 70 mg, $n = 5$ of each genotype), but the spleens were of similar size at 17–18 wk of age (90 vs 85 mg, $n = 4$).

Integrin $\alpha_D\beta_2$ is constitutively expressed by limited subsets of leukocytes in the absence of infectious challenge

A small population (<1%) of peripheral blood leukocytes from WT mice of C57BL/6, A/J, SJL/J, and Swiss backgrounds stained positively for $\alpha_D\beta_2$. Splenic macrophages were used as controls in the staining reactions (see below and Fig. 2, *E* and *F*). This feature was unexpected since other β_2 integrins are highly expressed on circulating mouse leukocytes and are involved in their emigration from the blood in response to inflammatory stimuli (5, 6) and because $\alpha_D\beta_2$ is more broadly displayed on human leukocytes (Ref. 8 and our unpublished observations). In previous studies, α_D was reported to be absent from circulating murine leukocytes (16) and to be present on only a small fraction of circulating canine leukocytes (30).

When we examined tissues, α_D staining was restricted to cells of the splenic red pulp, thymus, and bone marrow in adult WT C57BL/6 mice (Figs. 2 and 3 and Table I). By flow cytometry, α_D^+ splenocytes were positive for β_2 (CD18), as expected (1,3). $\alpha_D\beta_2$ is also expressed in rat splenic red pulp (data not shown) and in the red pulp of canine and human spleen (8,30), indicating that its localization in this domain is conserved across species. Scattered groups of cells in the bone marrow and thymus of WT mice express α_D at lower staining intensity compared with that in spleen but with similar cellular morphology (Table I and Fig. 2). These cells likely represent specific macrophage populations (see below). There was no staining of tissues from $\alpha_D^{-/-}$ mice, documenting specificity of the immunohistochemical reactions and null phenotype of the $\alpha_D^{-/-}$ animals (Table I, Fig. 3*F*, and data not shown).

Specific populations of splenic macrophages differentially express integrin $\alpha_D\beta_2$

When splenocytes were first sorted based on their display of F4/80, a determinant that identifies murine monocytes and subpopulations of macrophages in normal and inflamed tissues (20, 31,32), >80% were also positive for α_D (Fig. 3*C*). Consistent with the flow cytometric results, the majority of red pulp splenocytes costained for α_D and F4/80 (Fig. 3, *A*, *B*, and *K*), although a small number of cells were brightly positive for one or the other marker. We detected F4/80 in the absence of $\alpha_D\beta_2$ in WT liver Kupffer cells, alveolar macrophages, and peripheral blood monocytes (data not shown) and in red pulp splenocytes from $\alpha_D\beta_2^{-/-}$ mice (Fig. 3*F*), demonstrating differential regulation of the two surface factors.

The majority of α_D^+ red pulp splenocytes also stained for macrosialin (Fig. 3*D*), the murine ortholog of human CD68, confirming their identity as macrophages (20). CD68 and α_D are also coexpressed on a subset of macrophages in human atherosclerotic tissue (8). Costaining for MARCO, a scavenger receptor that identifies the splenic marginal zone macrophage, and MOMA-1, which identifies the marginal metallophilic macrophage (20,33), demonstrated distinct populations of cells and localization patterns (Fig. 3, *G* and *I*). Thus, $\alpha_D\beta_2$ is expressed

by a specific population of macrophages in the red pulp that is distinct from the marginal zone macrophage subsets. Each macrophage subtype has particular roles in blood surveillance, antimicrobial defense, and organization of splenic microarchitecture, and is influenced by unique differentiation and retention signals (34). Analysis of expression of other α subunits (α_M, α_L, α_X) indicated that $\alpha_D\beta_2$ is the dominant β_2 integrin heterodimer on red pulp macrophages (Fig. 3*E* and data not shown).

$\alpha_D\beta_2$ mediates adhesive interactions of splenic red pulp macrophages

The functions of $\alpha_D\beta_2$ in vivo are uncharacterized, although it is assumed to mediate adhesive interactions (1,3,6,8,10,11,16). We established a modified Stamper-Woodruff assay system (26,27) using sections of spleen from WT and α_D-deficient mice and suspensions of isolated splenocytes. Suspended F4/80-positive macrophages from spleens of $\alpha_D^{-/-}$ animals were much less adherent than those from WT mice (Fig. 4). In parallel, incubation of suspended F4/80-positive splenocytes from WT mice with Abs against α_D inhibited adhesion to WT spleen sections by 65–90%; in addition, an Ab against VCAM-1, a ligand for human $\alpha_D\beta_2$ (9,10), reduced adhesion by a mean of 22% (10–43%; $n = 2$, data not shown). These results demonstrate that $\alpha_D\beta_2$ mediates adhesive interactions of red pulp macrophages and that it may influence their distribution. Furthermore, although VCAM-1 appears to be a ligand for $\alpha_D\beta_2$ in mouse tissues, these experiments also indicate that there are additional binding partners on target spleen cells and/or matrix. Although $\alpha_D\beta_2$ mediates binding of a critical subset of splenic macrophages (Figs. 2–4), it is not required for establishment of the basal topography of the red and white pulp (34) of the adult murine spleen or for retention of macrophage subsets in the splenic red pulp (Fig. 3*F*).

$\alpha_D\beta_2$ expression is dynamically altered on inflamed macrophages in response to P. berghei challenge and is regulated by cytokine signaling

Because red pulp macrophages have major effector activities in blood-borne infection and antigenemia (33,34), we chose models of systemic infectious challenge to further characterize regulation and functions of $\alpha_D\beta_2$. The spleen, an anatomic interface between innate and acquired immune effector cells (34), is critical in experimental malaria in all animals studied and red pulp macrophages have unique roles in recognition and clearance of infected RBC (35,36). Macrophages in other organs are also activated as a consequence of recognition of PBRC and by inflammatory signals generated by the systemic infection (36–38). Therefore, we first examined $\alpha_D\beta_2$ distribution and function in experimental malaria.

The distribution of splenic macrophages was dramatically altered by challenge with intraerythrocytic *P. berghei*, a lethal rodent malarial strain that induces pathophysiologic features similar to those in severe human malaria (28,37–39). Spleens of the infected animals were also enlarged (data not shown). Serial examinations over 5–20 days after infection demonstrated progressive reorganization of the splenic architecture and extensive loss of geographic localization of α_D^+ and MARCO$^+$ macrophages (Fig. 3, *G*, *H*, *H′*, *K*, *L*, and *L′*, and data not shown). MARCO$^+$ cells were widely distributed in the red pulp of *P. berghei*-infected animals, in contrast to their strict compartmentalization in the marginal zone of the uninfected spleen (Fig. 3, *G*, *H*, and *H′*). Linear arrays of doubly stained α_D^+ and MARCO$^+$ macrophages were present in red pulp (Fig. 3, *H* and *H′*), whereas expression of α_D and MARCO was restricted under basal conditions (Fig. 3*G*). Functional characteristics of the new population of α_D^+ MARCO$^+$ macrophages are not yet completely defined. Nevertheless, these cells contained heme pigment deposits, consistent with erythrophagocytosis (data not shown). The topography of MOMA-1$^+$ macrophages was also altered (Fig. 3, *J* and *J′*). Redistribution of splenic leukocytes also occurs in infection with other malarial pathogens (40).

Parallel but distinct changes occurred in the liver, which is a target organ in *P. berghei* infection (29,41). No α_D^+ cells were detected in the livers of uninfected animals (Table I,Fig. 5*A*, and data not shown), indicating that murine Kupffer cells, a macrophage subset (20), do not basally express α_D. α_D is also absent from human and canine Kupffer cells (8,30). By day 10 of infection with *P. berghei*, a minor population of small α_D^+ cells was detected, primarily in the portal vein areas (Fig. 5*B*). These cells were macrosialin$^+$ but negative for F4/80, $\alpha_M\beta_2$, and $\alpha_X\beta_2$. By day 20, large α_D^+ cells with morphology similar to that of splenic red pulp macrophages were numerous, were found in both the portal and central vein areas (Fig. 5*C*), and were again negative for F4/80, $\alpha_M\beta_2$, and $\alpha_X\beta_2$ while being positive for macrosialin. They were associated with deposits of heme pigment (Fig. 5, *B* and *C*, *right panels*, and data not shown), indicating that these cells participate in erythrophagocytosis as do splenic macrophages. There was also progressive hepatocyte necrosis and hepatic inflammation in the 10- to 20-day interval (data not shown).

In parallel, we examined α_D expression by murine M1 myeloid cells, an established model of terminal differentiation of myeloid precursors to macrophages. Treatment of M1 cells with LIF or IL 6, which are multifunctional cytokines and inducers of hemopoietic cell differentiation, causes them to differentiate to macrophages and undergo growth arrest (24). Undifferentiated M1 cells expressed no or low levels of α_D mRNA and protein under basal conditions (Fig. 6, *A*, and *B*). LIF induced expression of α_D mRNA and protein over 4 days of differentiation (Fig. 6, *A–C*, and data not shown). The pattern of staining of α_D in clusters of differentiated M1 macrophages (Fig. 6*B*) was similar to that of macrophages in situ (Fig. 2). F4/80 was also up-regulated on M1 macrophages (data not shown). To determine whether IL-6, which is increased in the blood in experimental and clinical malaria (36), induces α_D expression, we incubated M1 cells with IL-6 (1–100 ng/ml) or LIF (50 U/ml) for 4 days. IL-6 induced α_D mRNA and protein expression in a concentration-dependent fashion with a maximal effect at 10 ng/ml. By immunocytochemistry, the staining pattern and number of cells positive for α_D were equivalent when M1 were stimulated with 10 ng/ml IL-6 or 50 U/ml LIF. These experiments demonstrate that α_D expression is regulated by cytokine-induced macrophage differentiation, providing a mechanism for its local induction on macrophage subsets in inflamed tissues such as the liver (Fig. 5).

Targeted deletion of α_D differentially influences survival in systemic infection with *P. berghei* and Salmonella

We found that targeted deletion of α_D alters survival in *P. berghei* infection in an unexpected fashion. In three separate experiments, all of the WT animals infected with *P. berghei* were dead at 30 days (Fig. 7*A*). In two of the experiments, each of 10 WT mice succumbed by days 27 and 21, respectively, whereas a total of 5 $\alpha_D^{-/-}$ animals (3 in experiment 1 and 2 in experiment 2) survived to day 30. A third experiment demonstrated an even more malignant course, with 9 of 10 WT animals dead by day 14 compared with 7 of 10 $\alpha_D^{-/-}$ animals; 1 $\alpha_D^{-/-}$ mouse survived until day 30. The difference between the cumulative survival curves for each genotype in these experiments (Fig. 7*A*) was highly significant ($p = 0.0059$). Thus, targeted deletion of α_D alters the natural history and increases survival in the first 30 days of infection in this model, a period in which all WT animals succumbed. To confirm that the survival advantage during this time span represents a biologic feature selectively imposed by deletion of $\alpha_D\beta_2$, we performed two experiments in which other genetically modified mice were examined as controls. In the first, mice deficient in TLR2 (10 animals) were infected with *P. berghei* in parallel with WT mice (10 animals). In the second, mice deficient in inducible NO synthase (iNOS) (15 animals) and WT mice (24 animals) were studied. All iNOS and TLR2 animals were dead by days 18 and 19, respectively, whereas mortality of the WT mice was similar to that shown in Fig. 7*A*, with a progressive decrease in the number of surviving animals to day 28. Thus, deletion of neither iNOS nor TLR2, innate immune factors that

influence the natural history of malaria (39), reproduced the mortality pattern imposed by genetic deletion of α_D in these studies (Fig. 7*A*).

The survival curves of WT and $\alpha_D^{-/-}$ mice diverged at days 8–10 after *P. berghei* infection and significantly more $\alpha_D^{-/-}$ animals were alive over the succeeding 3 wk (Fig. 7*A*). To begin to examine the mechanisms involved, we focused on the period of divergence and first examined erythrocyte parasite burden and magnitude of anemia, which are key determinants of outcome in severe malaria (36–39). Between days 10 and 21, the mice became hyperparasitemic and profoundly anemic but there were no consistent differences in samples from $\alpha_D^{-/-}$ and WT mice (Fig. 7, *B* and *C*), excluding differences in these two central mechanisms (39) as causes for the difference in survival (Fig. 7*A*). In addition, these results indicate that $\alpha_D\beta_2$ is not required for clearance of PRBC. The splenic microarchitecture is essential for rapid resolution of primary infection with *Plasmodium* species and influences key aspects of the host response (35,40). We found that the organization of splenic red and white pulp is dramatically altered in *P. berghei* infection (Fig. 3, *H*, *J*, and *L*). Nevertheless, this rearrangement of splenic architecture also occurred in $\alpha_D^{-/-}$ animals with loss of distinct boundaries between the red pulp and marginal zone. This indicated that differences in splenic macroarchitecture, which might occur due to alteration in adhesive properties of red pulp macrophages (Fig. 4) as a result of deletion of $\alpha_D\beta_2$, do not account for the differences in survival (Fig. 7*A*).

Systemic cytokines are proposed to be key regulators of the pathogenesis of complicated malaria (35,40). Therefore, we next performed an initial survey of multiple cytokines in the blood of three animals of each genotype at 10 days of infection using a multiplex screening assay. This analysis suggested diverse alterations in systemic levels of cytokines in $\alpha_D^{-/-}$ and WT mice, including variations in IL-12, IFN-γ, IL-6, MCP-1, and KC. To explore this initial finding further, we examined levels of IL-12 in serum samples from a second group of animals studied on day 10 of infection. We chose IL-12 as an initial candidate for further analysis because it is implicated in the pathogenesis of severe human malaria and has been identified as a mediator of tissue injury in lethal *P. berghei* infection (29,41). Consistent with the preliminary analysis, we found that IL-12 concentrations were lower in the blood of infected $\alpha_D^{-/-}$ mice compared with levels in samples from WT mice (Fig. 7*D*). Thus, alterations in the pattern and levels of inflammatory cytokines may contribute to the survival advantage in $\alpha_D^{-/-}$ animals in this phase of the systemic infection (Fig. 7*A*).

To further define the phenotype of α_D-deficient mice and to determine whether deletion of α_D has a stereotyped, or conversely, differential impact on systemic infections, we examined $\alpha_D^{-/-}$ and WT mice in a model of *S. typhimurium* sepsis. This model was chosen for comparison because, although it is a bacterial pathogen, it also involves blood-borne phases and clearance by splenic, hepatic, and marrow macrophages (35,44), features that are similar to *P. berghei* infection. A preliminary experiment (eight mice of each genotype) with 10^5 bacteria per inoculum suggested greater mortality in $\alpha_D^{-/-}$ animals. A second experiment with 10 animals of each genotype but with a 10-fold lower inoculum supported the initial result ($p = 0.008$). We then performed three additional experiments with 10 WT and 10 $\alpha_D^{-/-}$ mice, an inoculum of 10^5 *Salmonella*, and a 10-day study period in each. (The change in study period was required because of animal housing constraints.) These studies replicated the original finding and again documented greater mortality in the $\alpha_D\beta_2$-deficient animals (Fig. 8; $p = 0.0004$). Thus, survival patterns of $\alpha_D^{-/-}$ mice were clearly different in systemic infection with *P. berghei* (Fig. 7*A*) and *S. typhimurium* (Fig. 8). This difference in natural history demonstrates that the effect of genetic deletion of α_D in murine models of systemic infection varies with the nature of the pathogen, indicating specialized functions of integrin $\alpha_D\beta_2$ and the immune effector cells that express it in host defense against invading microbes.

Discussion

Leukocyte integrins have essential but incompletely defined activities in host defense and conserved functions in mice and humans (1–6). Our observations provide the first detailed characterization of $\alpha_D\beta_2$ in vivo, information that is currently lacking in the field (1,3), along with new insights into its regulation and functions. The studies clearly demonstrate that it has unique features in inflammation and host defense. Interestingly, although other β_2 integrins are highly expressed on circulating murine leukocytes and are critical in their trafficking from blood to tissues, $\alpha_D\beta_2$ is present on only a minor and as yet uncharacterized population of these cells in WT animals in naive conditions (see *Results*; Y. Miyazaki and G. A. Zimmerman, unpublished data). In contrast, $\alpha_D\beta_2$ is constitutively expressed on macrophages of splenic red pulp, bone marrow, and thymus of WT mice in the absence of infectious or inflammatory challenge (Table I and Figs. 2 and 3) indicating that, in this species, $\alpha_D\beta_2$ has major functions apart from emigration of leukocytes from the blood. We found that $\alpha_D\beta_2$ mediates adhesion of red pulp macrophages, identifying one of its extravascular activities and demonstrating a functional role for the $\alpha_D\beta_2$ heterodimer on macrophages for the first time. Previously, adhesive functions for $\alpha_D\beta_2$ have only been observed in human eosinophils and surrogate cell lines (8–11). We also found that in response to erythrocytic infection with a malarial pathogen, *P. berghei*, new and previously unrecognized populations of α_D^+ macrophages emerge in the spleen and liver, demonstrating dynamic regulation of $\alpha_D\beta_2$ in this cell type and illustrating the daedal nature of macrophage heterogeneity (42,43). In contrast, bacterial and immune challenge to the murine lung, another macrophage-rich organ, did not induce expression of α_D under several experimental conditions (Y. Miyazaki, H. Castro Faria Neto, and G. A. Zimmerman, unpublished data) and α_D was not increased on peritoneal macrophages in response to thioglycolate instillation (Table I). This indicates that selective signals are required for its display on macrophage subpopulations, pointing to context-specific functions of $\alpha_D\beta_2$. Targeted deletion of α_D unexpectedly yielded a survival advantage in lethal malarial infection. Conversely, deletion of α_D had the opposite effect in a model of *Salmonella* sepsis, indicating complex roles for $\alpha_D\beta_2$ in defense against systemic pathogens. The latter findings are consistent with both beneficial and injurious activities of leukocyte integrins (2,7) and macrophages (42,44) in innate immune responses.

The roles of leukocyte integrins in responses to microbial invasion are incompletely characterized, although this is clearly a chief defensive function of these specialized effector proteins (1,2,6). Targeted deletion of β_2, which causes deficiency of all leukocyte integrin heterodimers, increases susceptibility to many bacterial pathogens but affords resistance to *Listeria monocytogenes* and improves control of local infection by *Leishmania major*, a protozoan parasite of macrophages, in murine models (5,6). These patterns of susceptibility and resistance demonstrate complex functions of leukocyte integrins in innate and acquired immune responses to infection (6), a feature further indicated by variable contributions of individual heterodimers in specific experimental models (45,46). Participation of integrins in the pathobiology of complicated malaria is suggested (37), but largely unexplored. mAbs against α_L improved survival in models of cerebral malaria, suggesting a role for $\alpha_L\beta_2$ (LFA-1), whereas Abs against α_m or ICAM-1, a ligand for $\alpha_L\beta_2$, did not protect (47,48). In contrast to Ab administration, targeted deletion of ICAM-1 increased survival in a cerebral malaria model (49). A β_3 integrin (3) regulates the pattern of cytokines released by human macrophages and myeloid dendritic cells activated by PRBC (36); nevertheless, contributions of β_2 integrins to this process are undefined. Thus, the regulation and activities of leukocyte integrins in malarial infection are uncharacterized. We found extensive display of α_D on red pulp macrophages of the WT spleen (Figs. 2 and 3), suggesting that $\alpha_D\beta_2$ mediates responses to systemic pathogens (34), potentially including malarial parasites (35). We then explored this possibility using a model that mimics many features of severe human malaria, *P. berghei* infection (28,29,37–39).

Challenge of WT mice with intraerythrocytic *P. berghei* resulted in a dramatic alteration in the microarchitecture of the splenic red pulp and marginal zone with loss of demarcation of these regions and appearance of a new subset of α_D^+MARCO$^+$ macrophages (Fig. 3 and data not shown). The distribution and activities of splenic macrophages and other leukocytes influence the inflammatory and immune responses to malarial invaders and may alter susceptibility to concomitant infection by bacterial and viral pathogens (35,36,39,40,50,51). In lethal *P. falciparum* infection, the marginal zone is dramatically altered with almost complete histologic "dissolution" (50), similar to the microarchitectural disruption in *P. berghei* infection (Fig. 3). In parallel with changes in splenic microarchitecture and macrophage populations, a new subset of α_D^+ macrosialin$^+$ macrophages emerged in the livers of WT mice infected with *P. berghei* (Fig. 5). It is likely that these new macrophage subpopulations in spleen and liver mediate responses to malarial infection that are in some cases injurious or maladaptive (36,37,42,43). In addition, they clearly demonstrate dynamic expression of $\alpha_D\beta_2$ induced by pathogen challenge and inflammatory signals.

It is not clear whether new populations of $\alpha_D\beta_2$-expressing macrophages in the spleen and liver in *P. berghei* infection are due to migration, proliferation, and differentiation of blood leukocytes that express α_D or, conversely, to induction of $\alpha_D$on resident macrophages or macrophage precursors. To begin to explore this issue, we used the murine M1 myeloid cell model, in which agonist-induced macrophage differentiation can be dissociated from cellular proliferation (24). LIF and IL-6, which are multifunctional cytokines released into the blood in murine endotoxemia and, in the case of IL-6, malaria (37,38), trigger terminal differentiation of M1 cells to macrophages (24). We found that LIF and IL-6 induced new expression of α_D on M1 cell-derived macrophages, providing a potential mechanism for dynamic regulation of $\alpha_D\beta_2$ on specific macrophage subsets in tissues such as the liver or spleen in response to inflammatory signals (Figs. 3 and 5). As noted previously, unique patterns of cytokines or other signaling factors are likely required for the highly restricted expression of $\alpha_D\beta_2$ on individual macrophage subsets in healthy animals (Table I and Figs. 2 and 3) and changes in expression in response to inflammatory challenge (Figs. 3 and 5). Additional characterization of the minor subpopulation of α_D^+ blood leukocytes will be required to further define regulation of α_D on this subset and whether it is altered by signals for migration and/or proliferation.

Improved survival of $\alpha_D^{-/-}$ mice infected by *P. berghei* was unexpected and indicated that pathophysiologic events mediated by $\alpha_D\beta_2$ have deleterious consequences in lethal malarial infection. Although at first glance the survival advantage at 30 days appears relatively small, significant differences over an approximate 3-wk period represent a substantial benefit in a syndrome with 100% mortality (Fig. 7*A*). Mice infected with *P. berghei* die secondary to cerebral, hepatic, pulmonary, renal, and cardiac complications that are superimposed on hyperparasitemia and severe malarial anemia (28,29,37–39,41,52,53). The pathobiologic mechanisms that mediate systemic inflammation and critical organ injury in experimental and clinical malaria are complex and multifactorial, and their precise identification has remained elusive (36–39). One or multiple organ-specific or multiorgan components could be influenced by deletion of $\alpha_D\beta_2$. To begin to explore these possibilities, we first examined two key determinants of malarial pathogenesis, severe malarial anemia, and intraerythrocyte parasite burden (39). Splenic red pulp macrophages, which are rich in $\alpha_D\beta_2$ (Figs. 2 and 3 and Table I), are critical for removal of PRBC and for parasite killing, and changes in splenic function and splenectomy alter anemia parasitemia and outcomes (35,50,51). Profound anemia in murine malaria is due in part to hemolysis and hyperphagocytosis of infected and uninfected RBC by splenic red pulp and/or hepatic macrophages and to ineffective erythropoiesis (39, 52,53). The latter process is influenced by marrow macrophages (54,55) and, therefore, potentially by $\alpha_D\beta_2$ (Table I and Fig. 2). Nevertheless, we found similar numbers of PRBC and degrees of anemia in $\alpha_D^{-/-}$ and WT mice (Fig. 7, *B* and *C*), indicating that differences in intraerythrocytic parasite burden, clearance of PBRC by macrophage subsets, and ineffective

erythropoiesis are not the pivotal mechanisms that determined altered survival of $\alpha_D^{-/-}$ animals. In addition, we evaluated differences in splenic microarchitecture, which influences early and late host responses to malarial pathogens (36,40,50,51) (also see above). We found that dramatic alterations in red pulp and marginal zone topography, which were histologically similar to those reported in *P. falciparum* infection in humans (50), occurred in both WT and $\alpha_D^{-/-}$ animals (Fig. 3 and data not shown). Therefore, differences in this variable do not account for the survival advantage of $\alpha_D^{-/-}$ animals. In addition to hyperparasitemia, severe anemia, and splenic reorganization, cytoadhesive vasculopathy, in which PRBC adhere to endothelium and occlude microvessels of critical organs, is also a proposed mechanism of injury and death in severe malarial syndromes (37–39). We have not observed expression of $\alpha_D\beta_2$ on murine erythrocytes or endothelial cells (Table I and data not shown), consistent with the highly restricted distribution of leukocyte integrins (1,3), making it unlikely that altered interactions of PRBC with endothelium account for improved survival of $\alpha_D^{-/-}$ animals. Therefore our studies, in aggregate, excluded several major determinants of mortality in *P. berghei* infection and pointed to other mechanisms.

Cytokine signaling is central to the systemic manifestations of experimental and clinical malaria (37–39,53), and outside-in signals mediated by integrins both trigger and modify synthesis of cytokines by macrophages and monocytes (1,3,56–59). In preliminary studies, we found altered patterns of plasma cytokines in $\alpha_D^{-/-}$ mice infected with *P. berghei* compared with those in WT animals at 10 days after challenge. In additional assays to validate these preliminary data, we found that IL-12 levels in the blood of infected $\alpha_D\beta_2$-deficient mice were substantially lower than those in samples from WT controls (Fig. 7*D*). IL-12 signaling induces hepatic injury in lethal erythrocytic *P. berghei* infection (35,40), providing a rationale for examining this cytokine as a sentinel proinflammatory mediator under the conditions of our experiment. (Studies of additional cytokines are in progress.) Furthermore, synthesis of IL-12 by monocytes and macrophages is suppressed by engagement of β_2 integrins (57–59), suggesting a mechanism for its regulation under these conditions, although this has not yet been examined for $\alpha_D\beta_2$. Nevertheless, we do not propose decreased plasma levels of IL-12 as the sole mechanism for improved survival in $\alpha_D^{-/-}$ animals, since excesses of individual cytokines seem unlikely to account for all multiorgan and systemic manifestations of severe malarial syndromes (38,39). Furthermore, additional cellular complexity may be involved. $\alpha_D\beta_2$ influences responses of T cells, which are immune effectors in severe experimental malaria (37–39,60), and is reported to determine functional ontogeny of T lymphocytic subsets and their responses to microbial Ags (16).

To further characterize the phenotype of $\alpha_D^{-/-}$ animals in systemic infectious models and to determine whether the activities of $\alpha_D\beta_2$ are stereotyped regardless of the nature of the pathogen, we examined α_D-deficient mice in *S. typhimurium* infection. Macrophage activity, cytokine signaling, and immune cell interactions are central in responses to *Salmonella* invasion (44), as they are in malarial infection (36–39). Deletion of $\alpha_D\beta_2$ accelerated mortality in mice infected with *S. typhimurium*, in contrast to the survival pattern in infection with *P. berghei* (see *Results* and Fig. 8). The difference in outcomes in the *P. berghei* and *Salmonella* models may in part be due to recognition of *Salmonella* by splenic marginal zone macrophages rather than $\alpha_D\beta_2$-rich red pulp macrophages (35). Furthermore, endogenous IL-12 augments protective immune responses against *Salmonella* species (61), whereas it contributed to immune injury in *P. berghei* infection (29,41). Thus, the altered levels of IL-12 in $\alpha_D^{-/-}$ mice may partially account for the differences in survival in the two infectious challenges. In addition, however, different patterns of survival in the malaria and *Salmonella* models may also be due to different functional roles played by $\alpha_D\beta_2^+$ macrophage subsets in systemic infection by intracellular bacteria vs malarial parasites. It is not yet clear how effector characteristics of macrophages (42,43) govern the balance between defense and injury in *P. berghei* and *S. typhimurium* infections (44,62) or how $\alpha_D\beta_2$ influences activation patterns of

specific macrophage populations. Further delineation of mechanisms by which $\alpha_D\beta_2$ and other leukocyte integrins regulate the localization and functional repertoires of macrophage subsets (42) will clarify this issue. This information may then be useful in understanding the effects of innate immune events in humans infected by malaria and *Salmonella*, which together kill >2.5 million subjects each year worldwide (36,39,44,62). $\alpha_D\beta_2$ is expressed by leukocytes in human splenic red pulp (8) and is displayed in regulated fashion by primary human macrophages and dendritic cells (Y. Miyazaki, E. Harris, A. Shah, and G. A. Zimmerman, manuscript in preparation), suggesting that it has key roles in these and other human infectious syndromes.

Acknowledgements

We thank our laboratory staffs for technical assistance, Andressa Almeida for preparation of infectious agents for in vivo experiments, and Kate Anderson for skilled animal husbandry. Liping Chen made important contributions to the development of α_D-deficient mice before her untimely death. Diana Lim prepared the figures and graphic art and Mary Madsen, Adrienne Triplett, and Linn Steele contributed invaluable effort in preparation of this manuscript. We thank Leslie Ostler for performing specific experiments, Kelley Murphy for advice regarding immunocytochemical analysis, and Marga Massey for samples of rat spleen. Monica Van der Vieren, Patricia Hoffman, and Michael Gallatin of ICOS Corporation generously provided critical reagents, including key anti-α_D Abs and a murine α_D probe template for genomic library screening. We also thank colleagues in our group and Dr. Merle Sande for valuable discussions.

References

1. Harris ES, McIntyre TM, Prescott SM, Zimmerman GA. The leukocyte integrins. J Biol Chem 2000;275:23409–23412. [PubMed: 10801898]
2. Bunting M, Harris ES, McIntyre TM, Prescott SM, Zimmerman GA. Leukocyte adhesion deficiency syndromes: adhesion and tethering defects involving β_2 integrins and selectin ligands. Curr Opin Hematol 2002;9:30–35. [PubMed: 11753075]
3. Hynes RO. Integrins: bidirectional, allosteric signaling machines. Cell 2002;110:673–687. [PubMed: 12297042]
4. Scharffetter-Kochanek K, Lu H, Norman K, van Nood N, Munoz F, Grabbe S, McArthur M, Lorenzo I, Kaplan S, Ley K, et al. Spontaneous skin ulceration and defective T cell function in CD18 null mice. J Exp Med 1998;188:119–131. [PubMed: 9653089]
5. Etzioni A, Doerschuk CM, Harlan JM. Of man and mouse: leukocyte and endothelial adhesion molecule deficiencies. Blood 1999;94:3281–3288. [PubMed: 10552936]
6. Lee SH, Corry DB. Homing alone? CD18 in infectious and allergic disease. Trends Mol Med 2004;10:258–262. [PubMed: 15177189]
7. Yonekawa K, Harlan JM. Targeting leukocyte integrins in human diseases. J Leukocyte Biol 2005;77:129–140. [PubMed: 15548573]
8. Van der Vieren M, Le Trong H, Wood CL, Moore PF, St John T, Staunton DE, Gallatin WM. A novel leukointegrin, $\alpha_d\beta_2$, binds preferentially to ICAM-3. Immunity 1995;3:683–690. [PubMed: 8777714]
9. Grayson MH, Van der Vieren M, Sterbinsky SA, Michael Gallatin W, Hoffman PA, Staunton DE, Bochner BS. $\alpha_d\beta_2$ integrin is expressed on human eosinophils and functions as an alternative ligand for vascular cell adhesion molecule 1 (VCAM-1). J Exp Med 1998;188:2187–2191. [PubMed: 9841932]
10. Van der Vieren M, Crowe DT, Hoekstra D, Vazeux R, Hoffman PA, Grayson MH, Bochner BS, Gallatin WM, Staunton DE. The leukocyte integrin $\alpha_D\beta_2$ binds VCAM-1: evidence for a binding interface between I domain and VCAM-1. J Immunol 1999;163:1984–1990. [PubMed: 10438935]
11. Yakubenko VP, Yadav SP, Ugarova TP. Integrin αDβ2, an adhesion receptor up-regulated on macrophage foam cells, exhibits multiligand-binding properties. Blood 2006;107:1643–1650. [PubMed: 16239428]
12. El-Gabalawy H, Canvin J, Ma GM, Van der Vieren M, Hoffman P, Gallatin M, Wilkins J. Synovial distribution of α_d/CD18, a novel leukointegrin: comparison with other integrins and their ligands. Arthritis Rheum 1996;39:1913–1921. [PubMed: 8912515]

13. Noti JD. Expression of the myeloid-specific leukocyte integrin gene CD11d during macrophage foam cell differentiation and exposure to lipoproteins. Int J Mol Med 2002;10:721–727. [PubMed: 12429998]
14. Shanley TP, Warner RL, Crouch LD, Dietsch GN, Clark DL, O'Brien MM, Gallatin WM, Ward PA. Requirements for α_d in IgG immune complex-induced rat lung injury. J Immunol 1998;160:1014–1020. [PubMed: 9551942]
15. Oatway MA, Chen Y, Bruce JC, Dekaban GA, Weaver LC. Anti-CD11d integrin antibody treatment restores normal serotonergic projections to the dorsal, intermediate, and ventral horns of the injured spinal cord. J Neurosci 2005;25:637–647. [PubMed: 15659600]
16. Wu H, Rodgers JR, Perrard XY, Perrard JL, Prince JE, Abe Y, Davis BK, Dietsch G, Smith CW, Ballantyne CM. Deficiency of CD11b or CD11d results in reduced staphylococcal enterotoxin-induced T cell response and T cell phenotypic changes. J Immunol 2004;173:297–306. [PubMed: 15210787]
17. Bunting M, Bernstein KE, Greer JM, Capecchi MR, Thomas KR. Targeting genes for self-excision in the germ line. Genes Dev 1999;13:1524–1528. [PubMed: 10385621]
18. Mansour SL, Thomas KR, Capecchi MR. Disruption of the proto-oncogene int-2 in mouse embryo-derived stem cells: a general strategy for targeting mutations to non-selectable genes. Nature 1988;336:348–352. [PubMed: 3194019]
19. Schwenk F, Baron U, Rajewsky K. A cre-transgenic mouse strain for the ubiquitous deletion of loxP-flanked gene segments including deletion in germ cells. Nucleic Acids Res 1995;23:5080–5081. [PubMed: 8559668]
20. McKnight AJ, Gordon S. Membrane molecules as differentiation antigens of murine macrophages. Adv Immunol 1998;68:271–314. [PubMed: 9505092]
21. Cao Y, Murphy KJ, McIntyre TM, Zimmerman GA, Prescott SM. Expression of fatty acid-CoA ligase 4 during development and in brain. FEBS Lett 2000;467:263–267. [PubMed: 10675551]
22. Ohteki T, Maki C, Koyasu S. Overexpression of Bcl-2 differentially restores development of thymus-derived $CD4^{-}8^{+}$ T cells and intestinal intraepithelial T cells in IFN-regulatory factor-1-deficient mice. J Immunol 2001;166:6509–6513. [PubMed: 11359801]
23. Kessel JM, Hayflick J, Weyrich AS, Hoffman PA, Gallatin M, McIntyre TM, Prescott SM, Zimmerman GA. Coengagement of ICAM-3 and Fc receptors induces chemokine secretion and spreading by myeloid leukocytes. J Immunol 1998;160:5579–5587. [PubMed: 9605163]
24. Hoffman-Liebermann B, Liebermann DA. Interleukin-6- and leukemia inhibitory factor-induced terminal differentiation of myeloid leukemia cells is blocked at an intermediate stage by constitutive c-myc. Mol Cell Biol 1991;11:2375–2381. [PubMed: 1901940]
25. Pabla R, Weyrich AS, Dixon DA, Bray PF, McIntyre TM, Prescott SM, Zimmerman GA. Integrin-dependent control of translation: engagement of integrin $\alpha_{IIb}\beta_3$ regulates synthesis of proteins in activated human platelets. J Cell Biol 1999;144:175–184. [PubMed: 9885253]
26. Stamper HB Jr, Woodruff JJ. Lymphocyte homing into lymph nodes: in vitro demonstration of the selective affinity of recirculating lymphocytes for high-endothelial venules. J Exp Med 1976;144:828–833. [PubMed: 956727]
27. Yednock TA, Cannon C, Fritz LC, Sanchez-Madrid F, Steinman L, Karin N. Prevention of experimental autoimmune encephalomyelitis by antibodies against $\alpha_4\beta_1$ integrin. Nature 1992;356:63–66. [PubMed: 1538783]
28. Cordeiro RS, Cunha FQ, Filho JA, Flores CA, Vasconcelos HN, Martins MA. *Plasmodium berghei*: physiopathological changes during infections in mice. Ann Trop Med Parasitol 1983;77:455–465. [PubMed: 6362586]
29. Adachi K, Tsutsui H, Kashiwamura S, Seki E, Nakano H, Takeuchi O, Takeda K, Okumura K, Van Kaer L, Okamura H, et al. *Plasmodium berghei* infection in mice induces liver injury by an IL-12- and Toll-like receptor/myeloid differentiation factor 88-dependent mechanism. J Immunol 2001;167:5928–5934. [PubMed: 11698470]
30. Danilenko DM, Rossitto PV, Van der Vieren M, Le Trong H, McDonough SP, Affolter VK, Moore PF. A novel canine leukointegrin, $\alpha_d\beta_2$, is expressed by specific macrophage subpopulations in tissue and a minor $CD8^{+}$ lymphocyte subpopulation in peripheral blood. J Immunol 1995;155:35–44. [PubMed: 7541420]

31. Geissmann F, Jung S, Littman DR. Blood monocytes consist of two principal subsets with distinct migratory properties. Immunity 2003;19:71–82. [PubMed: 12871640]
32. Randolph GJ, Beaulieu S, Lebecque S, Steinman RM, Muller WA. Differentiation of monocytes into dendritic cells in a model of transendothelial trafficking. Science 1998;282:480–483. [PubMed: 9774276]
33. Van der Laan LJ, Dopp EA, Haworth R, Pikkarainen T, Kangas M, Elomaa O, Dijkstra CD, Gordon S, Tryggvason K, Kraal G. Regulation and functional involvement of macrophage scavenger receptor MARCO in clearance of bacteria in vivo. J Immunol 1999;162:939–947. [PubMed: 9916718]
34. Mebius RE, Kraal G. Structure and function of the spleen. Nat Rev Immunol 2005;5:606–616. [PubMed: 16056254]
35. Yadava A, Kumar S, Dvorak JA, Milon G, Miller LH. Trafficking of *Plasmodium chabaudi adami*-infected erythrocytes within the mouse spleen. Proc Natl Acad Sci USA 1996;93:4595–4599. [PubMed: 8643449]
36. Urban BC, Roberts DJ. Malaria, monocytes, macrophages, and myeloid dendritic cells: sticking of infected erythrocytes switches off host cells. Curr Opin Immunol 2002;14:458–465. [PubMed: 12088680]
37. de Souza JB, Riley EM. Cerebral malaria: the contribution of studies in animal models to our understanding of immunopathogenesis. Microbes Infect 2002;4:291–300. [PubMed: 11909739]
38. Hunt NH, Grau GE. Cytokines: accelerators and brakes in the pathogenesis of cerebral malaria. Trends Immunol 2003;24:491–499. [PubMed: 12967673]
39. Schofield L. Intravascular infiltrates and organ-specific inflammation in malaria pathogenesis. Immunol Cell Biol 2007;85:130–137. [PubMed: 17344907]
40. Beattie L, Engwerda CR, Wykes M, Good MF. $CD8^+$ T lymphocyte-mediated loss of marginal metallophilic macrophages following infection with *Plasmodium chabaudi chabaudi* AS. J Immunol 2006;177:2518–2526. [PubMed: 16888013]
41. Yoshimoto T, Takahama Y, Wang CR, Yoneto T, Waki S, Nariuchi H. A pathogenic role of IL-12 in blood-stage murine malaria lethal strain *Plasmodium berghei* NK65 infection. J Immunol 1998;160:5500–5505. [PubMed: 9605153]
42. Gordon S. Alternative activation of macrophages. Nat Immunol 2002;3:23–35.
43. Noel W, Raes G, Hassanzadeh Ghassabeh G, De Baetselier P, Beschin A. Alternatively activated macrophages during parasite infections. Trends Parasitol 2004;20:126–133. [PubMed: 15036034]
44. Wijburg OL, Simmons CP, van Rooijen N, Strugnell RA. Dual role for macrophages in vivo in pathogenesis and control of murine *Salmonella enterica* var. *Typhimurium* infections. Eur J Immunol 2000;30:944–953. [PubMed: 10741413]
45. Guerau-de-Arellano M, Alroy J, Bullard D, Huber BT. Aggravated Lyme carditis in $CD11a^{-/-}$ and $CD11c^{-/-}$ mice. Infect Immun 2005;73:7637–7643. [PubMed: 16239568]
46. Ghosh S, Chackerian AA, Parker CM, Ballantyne CM, Behar SM. The LFA-1 adhesion molecule is required for protective immunity during pulmonary *Mycobacterium tuberculosis* infection. J Immunol 2006;176:4914–4922. [PubMed: 16585587]
47. Grau GE, Pointaire P, Piguet PF, Vesin C, Rosen H, Stamenkovic I, Takei F, Vassalli P. Late administration of monoclonal antibody to leukocyte function-antigen 1 abrogates incipient murine cerebral malaria. Eur J Immunol 1991;21:2265–2267. [PubMed: 1679717]
48. Falanga PB, Butcher EC. Late treatment with anti-LFA-1 (CD11a) antibody prevents cerebral malaria in a mouse model. Eur J Immunol 1991;21:2259–2263. [PubMed: 1679716]
49. Favre N, Da Laperousaz C, Ryffel B, Weiss NA, Imhof BA, Rudin W, Lucas R, Piguet PF. Role of ICAM-1 (CD54) in the development of murine cerebral malaria. Microbes Infect 1999;1:961–968. [PubMed: 10617927]
50. Urban BC, Hien TT, Day NP, Phu NH, Roberts R, Pongponratn E, Jones M, Mai NT, Bethell D, Turner GD, et al. Fatal *Plasmodium falciparum* malaria causes specific patterns of splenic architectural disorganization. Infect Immun 2005;73:1986–1994. [PubMed: 15784539]
51. Weiss L. Mechanisms of splenic control of murine malaria: cellular reactions of the spleen in lethal (strain 17XL) *Plasmodium yoelii* malaria in BALB/c mice, and the consequences of pre-infective splenectomy. Am J Trop Med Hyg 1989;41:144–160. [PubMed: 2476037]

52. Evans KJ, Hansen DS, van Rooijen N, Buckingham LA, Schofield L. Severe malarial anemia of low parasite burden in rodent models results from accelerated clearance of uninfected erythrocytes. Blood 2006;107:1192–1199. [PubMed: 16210332]

53. McDevitt MA, Xie J, Shanmugasundaram G, Griffith J, Liu A, McDonald C, Thuma P, Gordeuk VR, Metz CN, Mitchell R, et al. A critical role for the host mediator macrophage migration inhibitory factor in the pathogenesis of malarial anemia. J Exp Med 2006;203:1185–1196. [PubMed: 16636133]

54. Yoshida H, Kawane K, Koike M, Mori Y, Uchiyama Y, Nagata S. Phosphatidylserine-dependent engulfment by macrophages of nuclei from erythroid precursor cells. Nature 2005;437:754–758. [PubMed: 16193055]

55. Soni S, Bala S, Gwynn B, Sahr KE, Peters LL, Hanspal M. Absence of erythroblast macrophage protein (Emp) leads to failure of erythroblast nuclear extrusion. J Biol Chem 2006;281:20181–20189. [PubMed: 16707498]

56. Rosales C, Juliano RL. Signal transduction by cell adhesion receptors in leukocytes. J Leukocyte Biol 1995;57:189–198. [PubMed: 7852832]

57. Marth T, Kelsall BL. Regulation of interleukin-12 by complement receptor 3 signaling. J Exp Med 1997;185:1987–1995. [PubMed: 9166428]

58. Mosser DM, Karp CL. Receptor mediated subversion of macrophage cytokine production by intracellular pathogens. Curr Opin Immunol 1999;11:406–411. [PubMed: 10448139]

59. Sutterwala FS, Noel GJ, Clynes R, Mosser DM. Selective suppression of interleukin-12 induction after macrophage receptor ligation. J Exp Med 1997;185:1977–1985. [PubMed: 9166427]

60. Jacobs T, Plate T, Gaworski I, Fleischer B. CTLA-4-dependent mechanisms prevent T cell induced-liver pathology during the erythrocyte stage of *Plasmodium berghei* malaria. Eur J Immunol 2004;34:972–980. [PubMed: 15048707]

61. Kincy-Cain T, Clements JD, Bost KL. Endogenous and exogenous interleukin-12 augment the protective immune response in mice orally challenged with *Salmonella dublin*. Infect Immun 1996;64:1437–1440. [PubMed: 8606114]

62. Stevenson MM, Riley EM. Innate immunity to malaria. Nat Rev Immunol 2004;4:169–180. [PubMed: 15039754]

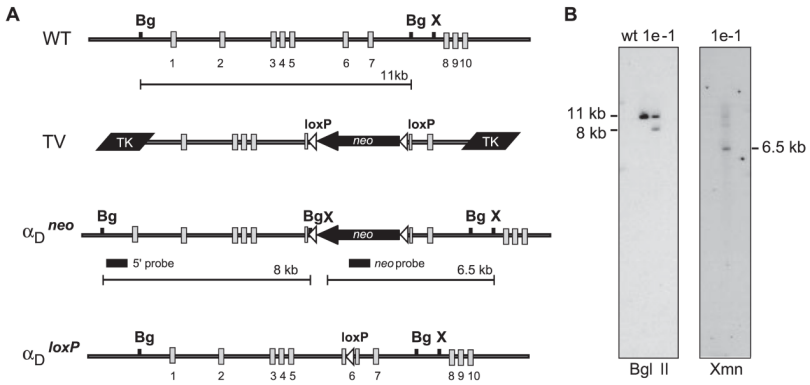

FIGURE 1.

Functional disruption of α_D by homologous recombination. *A*, The murine α_D genomic locus containing exons 1–10 is represented (WT). Genomic clones were isolated from a 129Sv mouse genomic λ DNA library using oligonucleotide probes specific to the α_D I domain. The largest (clone 3.1) was 14 kb in length and contained exons 1–6 as determined by Southern blot analysis and nucleic acid sequencing. A second 10-kb genomic clone (4.1) that overlapped with the 3′ end of 3.1 and contained exons 6–10 was also isolated. A 7.5-kb genomic fragment containing exons 1–5 and a 5′ region of exon 6 were cloned from 3.1 and inserted upstream of three in-frame stop codons in a polylinker modified pBlueScript vector. A 3-kb *Xmn*1-*Bgl*II fragment containing the 3′ end of exons 6 and 7 was cloned downstream of this fragment to generate a novel α_D allele leading to termination of translation in the I domain following residue 153(Ile). The novel α_D allele was cloned between two herpes simplex TK genes and a floxed neomycin selection cassette was inserted 3′ to the stop codons in exon 6 to generate the targeting vector. The targeting vector was linearized with *Xho*I and electroporated into TC1 embryonic stem cells. Recombinant embryonic stem cells were selected in the presence of G418 and FIAU as previously described (18) and were identified by Southern blot analysis using *Bgl*II and a 5′ flanking *Bam*Hi/*Bgl*II probe located outside the targeted region. Positive cell lines were confirmed using *Xmn*I digestion and hybridization to a probe corresponding to the neomycin gene. A single recombinant cell line (1e-1) was used for blastocyst injection to create recombinant mice. The floxed neomycin selection cassette was removed by mating to a transgenic mouse line that expresses Cre recombinase (19). Mice containing α_D^{loxP} and WT alleles were genotyped by PCR using isolated tail DNA. The forward (5′-GGACCCCAGGACACAGTTGAG-3′) and reverse (5′-CACAGGCCACAGTGTACAGTATT-3′) primers amplify a 268-bp band including the inserted loxP site from the recombinant allele and 215 bp from the WT allele. The recombinant mouse line was subsequently backcrossed and maintained on a C57BL/6 background. *B*, Southern blot analysis of genomic DNA isolated from WT embryonic stem cells and the α_D-recombinant embryonic stem cell line (1e-1). Genomic DNA digested with *Bgl*II was probed with a 600-bp *Bam*H1-*Bgl*II fragment from the α_D genomic clone. This 5′ probe hybridized to both the 11-kb fragment derived from the WT allele and the 8-kb fragment corresponding to the recombinant allele. The genomic structure of the 3′ end of the α_D^{neo} allele was confirmed in the 1e-1 clone by hybridization of the targeting vector-specific neomycin probe to the 6.5-kb *Xmn*I genomic fragment.

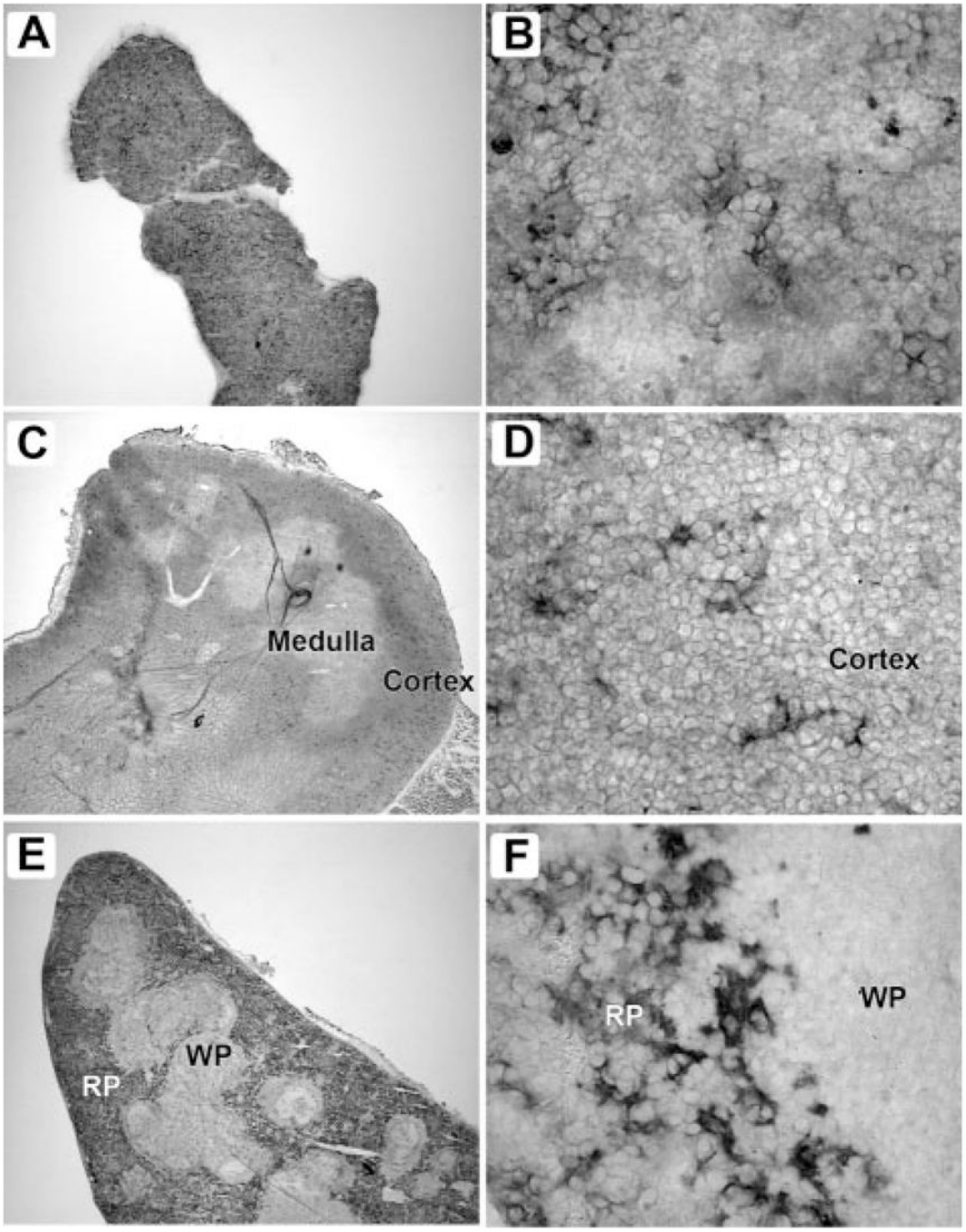

FIGURE 2.

$\alpha_D\beta_2$ is expressed by distinct populations of macrophages in bone marrow, thymus, and spleen. Frozen sections of freshly isolated tissues were stained with mAb 205c using an immunoperoxidase detection method. Tissues from 8- to 12-wk-old C57BL/6 mice were frozen in Tissue-Tek (Sakura Finetek) and 8-μm cryostat sections were deposited on Superfrost Plus slides (Fisher Scientific). The sections were then fixed in cold acetone for 10 min. Endogenous tissue peroxidase was eliminated by incubation with 0.01% hydrogen peroxide for 15 min. The sections were blocked by incubating with 5% normal goat serum, 1% BSA and avidin solution (Vector Laboratories) for 30 min, and primary Abs (hamster mAbs 205c or 279f raised against mouse α_D) were applied to the slides and incubated overnight at 4°C. A secondary Ab (biotin-

conjugated goat anti-hamster; Jackson ImmunoResearch Laboratories) was applied at a 1/1000 dilution and incubated for 30 min. Negative controls were performed by omitting the primary Ab or by applying an irrelevant isotype-matched primary Ab as a control. ABC reagent was prepared according to the manufacturer's instructions (Vector Laboratories) and applied to the sections for 30 min. Staining was developed using a NovaRed kit (Vector Laboratories), followed by counterstaining with Gill's hematoxylin, dehydration, and mounting using Cytoseal 60 medium (VWR). In each pair of figures, the panel on the *left* is magnified ×40 and on the *right* ×800. These distributions of α_D are representative of multiple studies. *A* and *B*, Bone marrow; *C* and *D*, thymus; *E* and *F*, spleen; WP, white pulp; RP, red pulp.

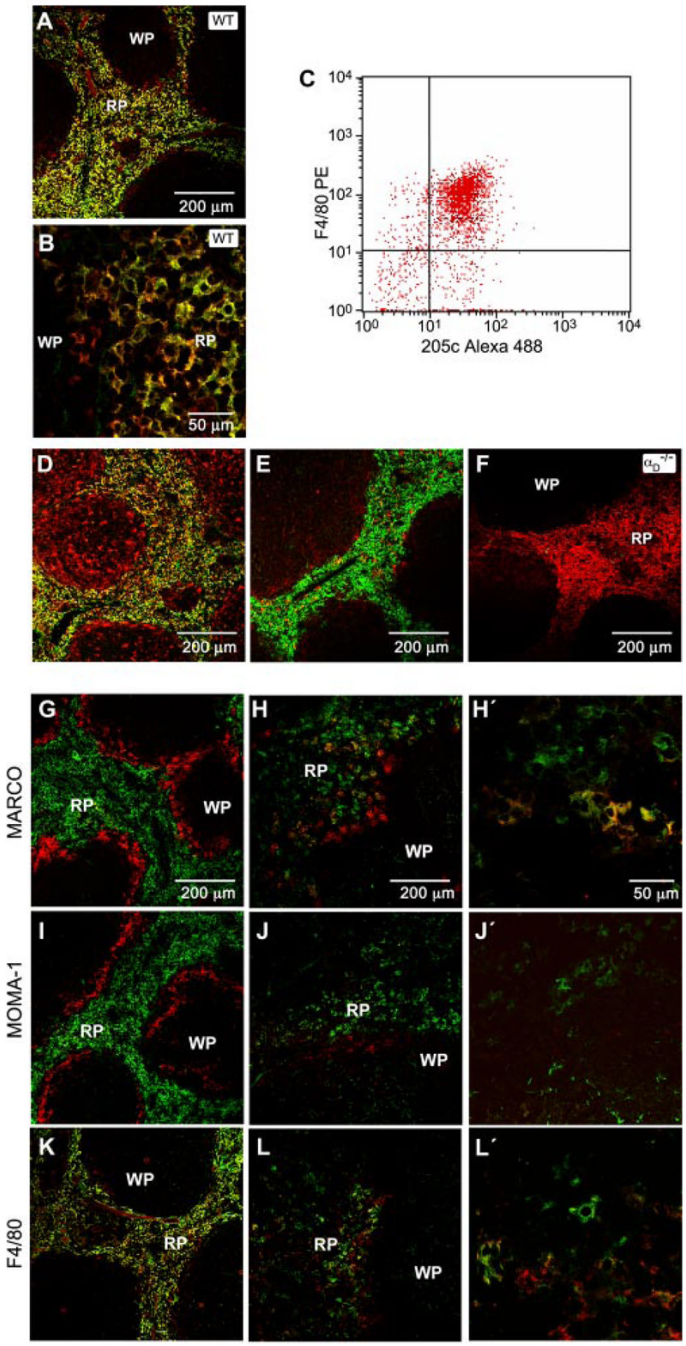

FIGURE 3.

$\alpha_D\beta_2$ is expressed by a unique population of splenic red pulp macrophages that is altered in *P. berghei* infection. Frozen sections of freshly isolated spleen from WT mice were costained using anti-α_D mAb (mAb 205c, green fluorescent labeling) and mAb against F4/80 (*A* and *B*), macrosialin (*D*), or α_m (*E*; red labeling). *F*, Spleen sections from $\alpha_D^{-/-}$ mice were costained for α_D and F4/80 as in *A* and *B*. The staining patterns shown are representative of tissue from multiple WT and $\alpha_D^{-/-}$ mice. *C*, Splenocytes were selected based on binding of PE-labeled anti-F4/80 and examined for expression of α_D by flow cytometry using mAb 205c conjugated to Alexa 488. A similar pattern was seen in two additional experiments. *G–L*, Frozen sections of spleen from control (*G*, *I*, and *K*) or *P. berghei*-infected (7 days postinfection; *H*, *J*, and *L*)

WT mice were costained for α_D and MARCO, MOMA-1, or F4/80. In each set of panels, α_D was detected by green fluorescence and the second marker was detected by red fluorescence. The *right panels* (*H′*, *J′*, and *L′*) show higher magnification detail. The staining patterns were similar in tissue from three infected animals. RP, Red pulp; WP, white pulp.

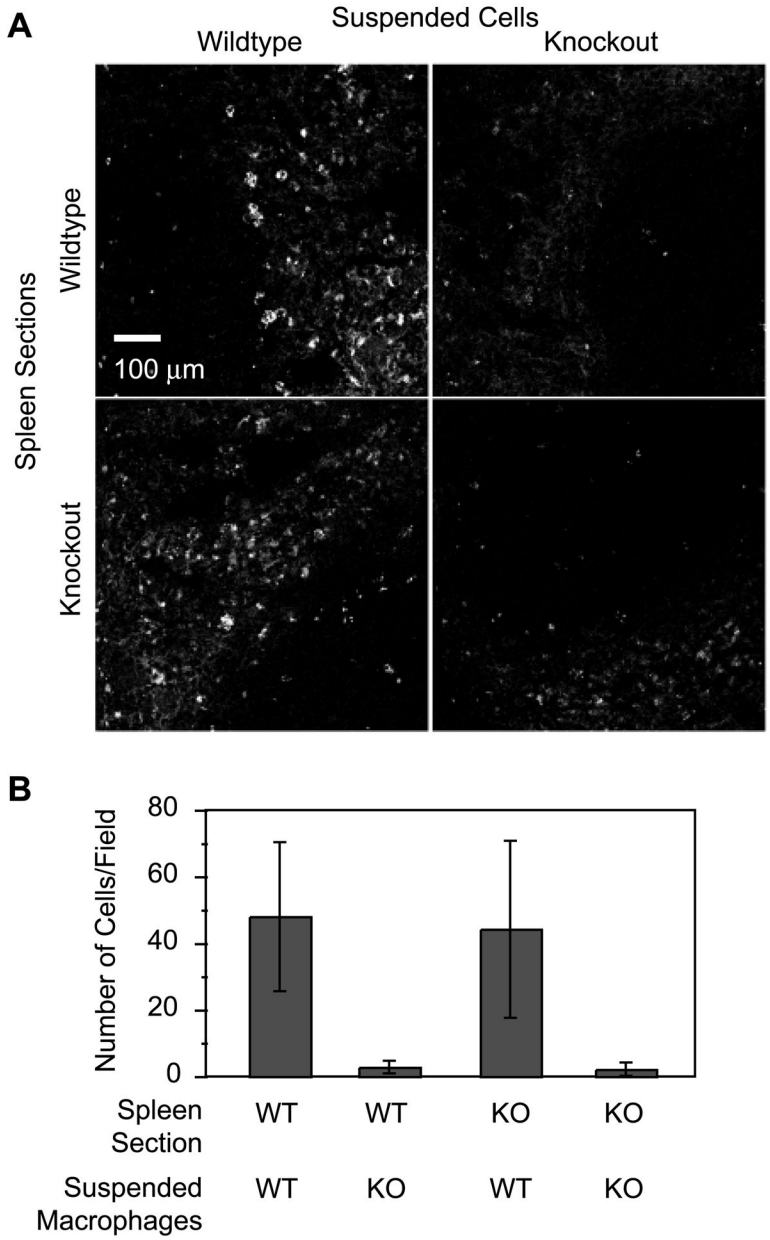

FIGURE 4.

Integrin $\alpha_D\beta_2$ mediates adhesive interactions of splenic red pulp macrophages. Suspensions of PE-labeled F4/80-positive macrophages (suspended cells) from WT or $\alpha_D^{-/-}$ (knockout (KO)) mice were incubated with spleen sections from WT or $\alpha_D^{-/-}$ animals, and the adherent splenocytes were imaged (*A*) and counted (*B*) as described in *Materials and Methods. A* and *B,* Representative of three separate experiments.

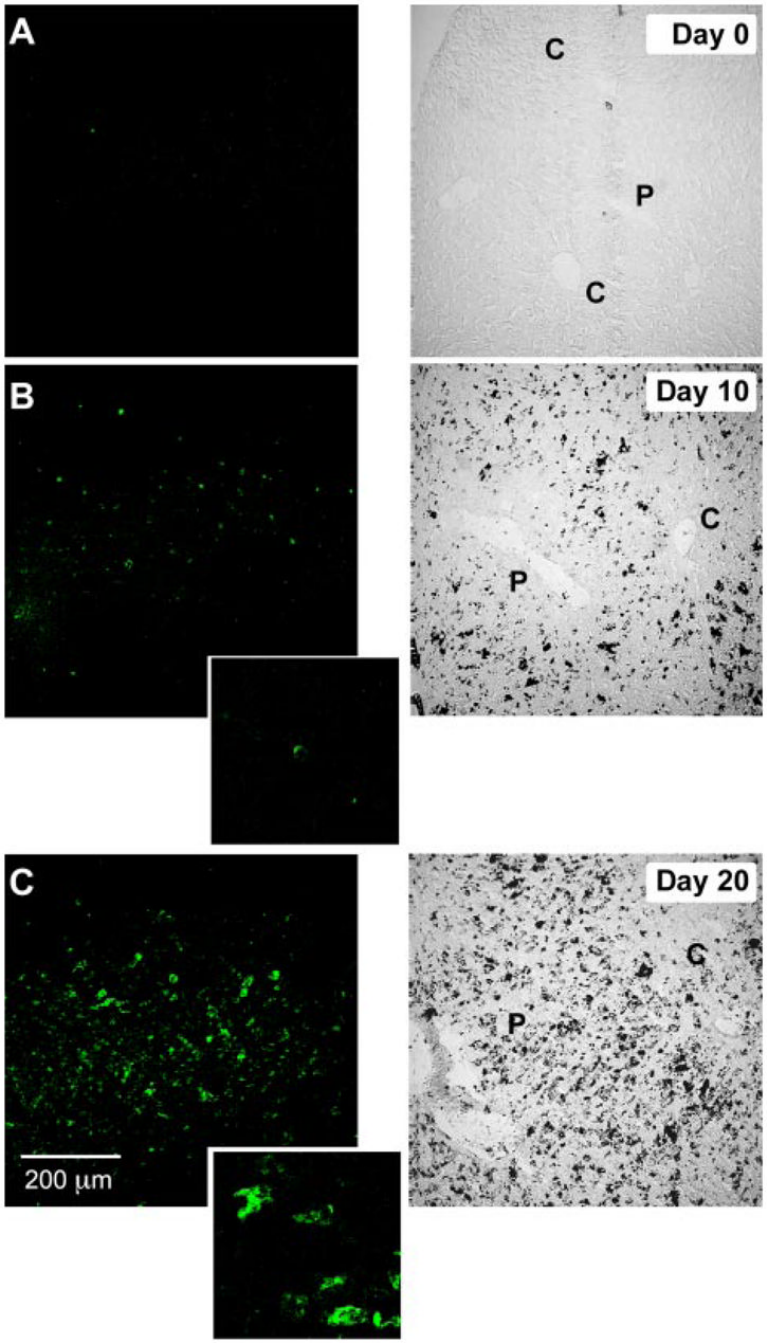

FIGURE 5.

New populations of α_D^+ macrophages are induced in the livers of mice infected with *P. berghei*. Control mice or animals infected with *P. berghei* were sacrificed at day 0 (*A*; control), day 10 (*B*), or day 20 (*C*) followed by staining for $\alpha_D\beta_2$ with immunofluorescent detection (mAb 205c). Transmitted light images are shown in the *right* panels for comparison. Original magnification, ×200; ×1200 in *inset*s in *B* and *C*. The black deposits in the *right panels* of *B* and *C* are heme pigments. The patterns shown are representative of those in liver tissue from three mice. C, Central vein; P, portal vein.

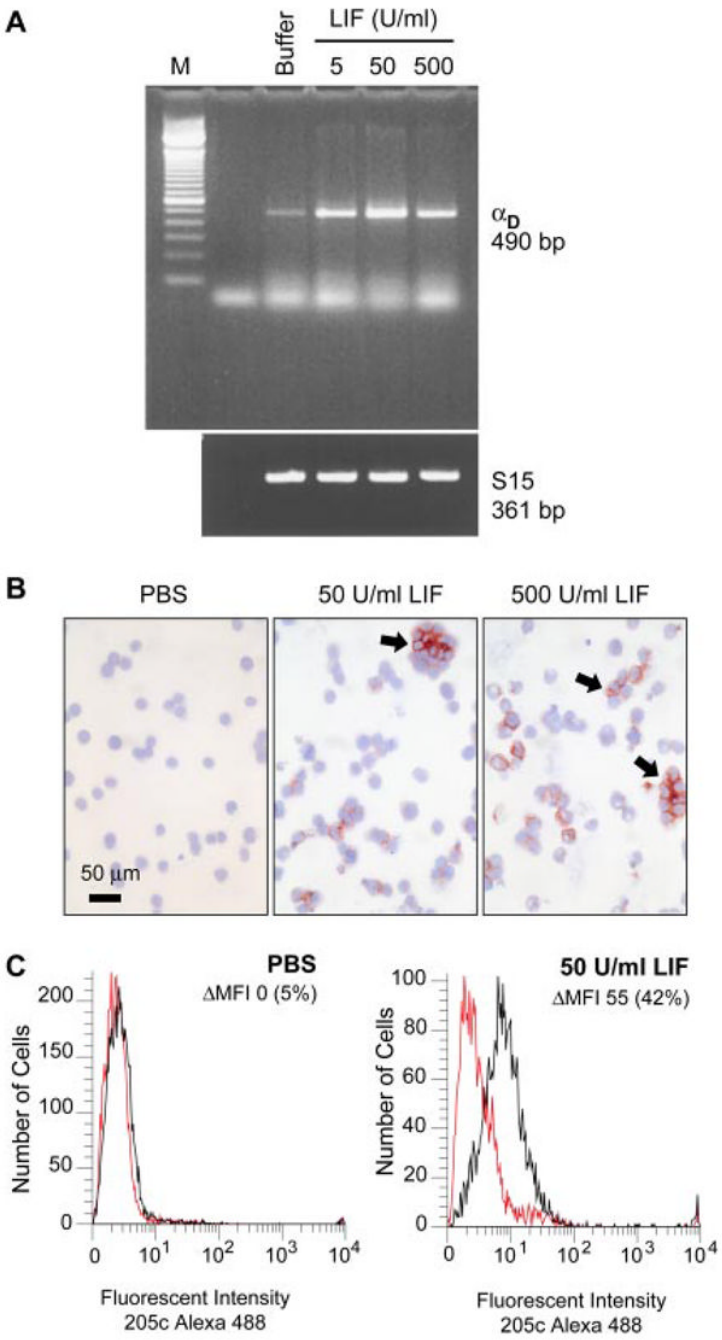

FIGURE 6.

Cytokine-mediated differentiation of macrophage precursors induces expression of α_D. M1 myeloid cells were cultured in the presence of the indicated concentrations of LIF for 4 days and then examined for expression of α_D. *A*, mRNA was isolated and probed for the α_D transcript by PCR. S15 served as a control for loading. *B*, Expression of α_D protein was assayed by incubation with mAb 205c and detection with an alkaline phosphatase-labeled secondary Ab (arrows). *C*, M1 cells were cultured with PBS or LIF as additives to the medium for 4 days and analyzed for surface expression of $\alpha_D\beta_2$ by flow cytometry using Alexa 488-conjugated mAb 205c to detect α_D (red tracings, control Ab; black tracings, mAb 205c). Change in mean

fluorescent intensity is denoted by ΔMFI. These results are representative of three additional studies.

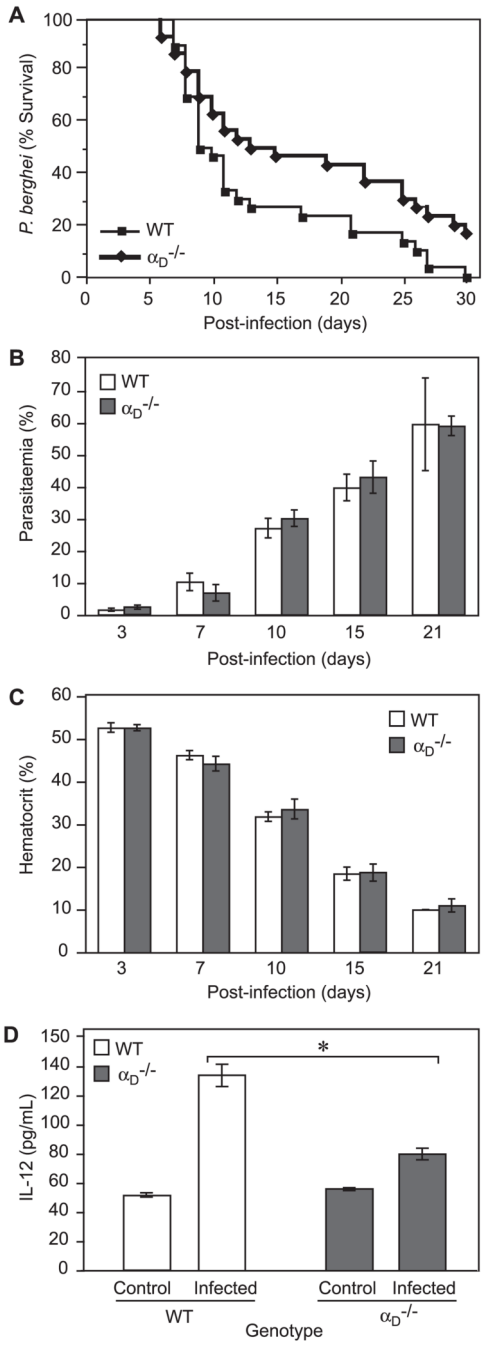

FIGURE 7.

Deletion of α_D provides a survival advantage in *P. berghei* infection. *A*, Mice were infected by i.p. challenge with *P. berghei* PRBC. Three separate experiments, each involving 10 WT and 10 $\alpha_D^{-/-}$ animals, were accomplished and the pooled results were analyzed. The difference between the cumulative survival curves was significant ($p = 0.0059$). B and *C*, The percentage of RBC infected by *P. berghei* was determined by microscopy and the hematocrit by RBC sedimentation. *B*, Results from one of three experiments and *C*, results from one of two experiments. Samples from variable numbers of surviving animals were studied at each time point. *D*, Serum samples were collected from WT control mice ($n = 5$), WT animals infected with *P. berghei* ($n = 10$), $\alpha_D^{-/-}$ control mice ($n = 8$), and *P. berghei*-infected $\alpha_D^{-/-}$ animals

($n = 7$) at 10 days after i.p. inoculation with PRBC. IL-12(p 40) concentrations were measured by ELISA. The differences between levels in samples from infected WT and $\alpha_D^{-/-}$ mice (*) was highly significant ($p < 0.0001$).

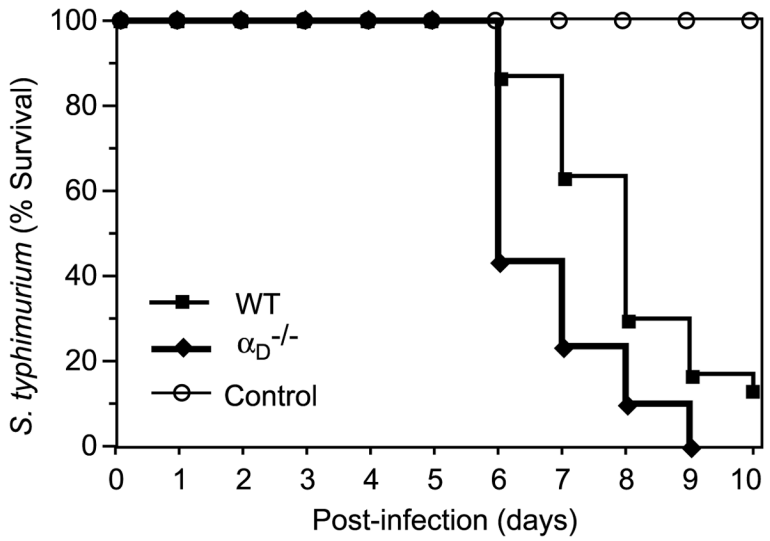

FIGURE 8.

Mortality is accelerated in $\alpha_D\beta_2$-deficient mice infected with *S. typhimurium*. WT or $\alpha_D^{-/-}$ mice were infected with *S. typhimurium* by the i.p. route (10^5 bacteria/animal). Groups of 10 $\alpha_D^{-/-}$ and 10 WT animals were studied in each of three separate experiments. The pooled survival data for 30 animals of each genotype are shown. The difference between the cumulative survival plots was significant ($p = 0.0004$). Control sham-infected mice that received vehicle alone were studied in parallel; no sham-infected animals died.

Table I

$\alpha_D\beta_2$ is restricted to macrophages in a limited number of tissues in WT C57BL/6 mice in the absence of infection or inflammation and is absent in $\alpha_D^{-/-}$ animals[a]

Tissue	Samples from WT Mice	Samples from $\alpha_D^{-/-}$ Mice
Lung	0	0
Thoracic lymph node	0	0
Liver	0	0
Kidney	0	0
Peyer's patch (gut)	0	0
Alveolar macrophages	0	ND
Brain	0	0
Skin	0	0
Spleen	++++	0
Thymus	++	0
Bone marrow	++	0
Blood leukocytes	0–+	0
Peritoneal macrophages	0–+	ND

[a]The levels of $\alpha_D\beta_2$ expression analyzed by immunocytochemistry were estimated based on staining intensity as strong (++++), intermediate (++), weak (0–+), or absent (0). In tissues with positive staining, $\alpha_D\beta_2$ was expressed by specific cells with morphologic characteristics of macrophages (see text and Figs. 2 and 3). These results summarize the findings in analysis of samples from multiple animals. Alveolar macrophages were obtained by bronchoalveolar lavage ($n = 2$). Resident peritoneal macrophages collected in the absence of agonist stimulation were largely negative for $\alpha_D\beta_2$, a feature that was confirmed by flow cytometry (0.23–4.7% of cells positive for α_D, $n = 4$). Expression of α_D was not increased in peritoneal macrophages at 48 h after thioglycolate injection into the peritoneal cavity as assayed by flow cytometry ($n = 3$).